

Supporting Information

Noninvasive Visualization of Respiratory Viral Infection Using Bioorthogonal conjugated Near-Infrared Emitting Quantum Dots

Hong Pan^{1†}, Pengfei Zhang^{1†}, Duyang Gao¹, Yijuan Zhang¹, Ping Li¹, Lanlan Liu¹, Ce Wang¹,
Hanzhong Wang², Yifan Ma^{1*} and Lintao Cai^{1*}

¹Guangdong Key Laboratory of Nanomedicine, CAS Key Laboratory of Health Informatics, Institute of Biomedicine and Biotechnology, Shenzhen Institutes of Advanced Technology, Chinese Academy of Sciences, Shenzhen, 518055, P. R. China

²State Key Laboratory of Virology, Wuhan Institute of Virology, Chinese Academy of Sciences, Wuhan, 430071, P. R. China

[†] These authors contributed equally to this paper.

^{*} Corresponding Authors: lt.cai@siat.ac.cn, yf.ma@siat.ac.cn

METHODS

Quantum Yield (QY) of QDs

The QY of N₃-QDs was measured using indocyanine green (ICG) as a standard (13.2% in DMSO). Solutions of N₃-QDs in PBS and dye in DMSO were optically matched at the excitation wavelength. Fluorescence spectra of N₃-QDs and ICG dye were taken under identical spectrometer conditions in triplicate and averaged. The optical density was kept below 0.1 at the λ max, and the integrated intensities of the emission spectra, corrected for differences in index of refraction and concentration, were used to calculate the quantum yields using the following equation:

$$QY_{QDs} = QY_{dye} \frac{I_{QDs}}{I_{dye}} \frac{A_{dye}}{A_{QDs}} \frac{n_{QDs}^2}{n_{dye}^2}$$

Where $n_{QDs,dye}$ is the refractive index, $A_{QDs,dye}$ is the absorption and $I_{QDs,dye}$ is the integrated fluorescence signal for the QDs and dye solutions, respectively.

The Stability of QD-Labeled H5N1 Pseudotypedviral Particles (QD-H5N1p)

QD-H5N1p was incubated with PBS, oseltamivir carboxylate (8 μ mol/L), mouse antiserum against H5N1p (1:1000), or negative serum for 2 h. The corresponding hydrodynamic diameter and PL intensity of the samples were measured by Malvern Zetasizer Nano ZS instrument and Edinburgh F900 fluorescent spectrometer after incubation, respectively.

The Stability of QDs in the Endosomes/Lysosomes

A549 cells were pretreated with or without 25 μ M chloroquine (CQ) for 1 h, followed by infection

with QD-labeled H5N1p. After 24 h post infection, the fluorescent images and the spectrum of QDs were recorded using multispectral fluorescence microscopy.

The effect of Antiviral Agents on the Infectivity of QD-H5N1p *in vitro*

HEK293T cells were infected with H5N1p, DBCO-H5N1p, or QD-H5N1p with or without the pretreatment of oseltamivir (8 $\mu\text{mol/L}$) or mouse antiserum against H5N1p (1:1000) at 37°C for 0.5 h. Cells were washed with PBS for twice to remove the unbounded QD-H5N1p and the fluorescence images were recorded using a multiple fluorescence microscopy. At 24 h after infection, the infectivity of viral particles was determined by measuring the percentage of GFP⁺ cells using flow cytometry.

Real-Time Polymerase Chain Reaction (RT-PCR) Analysis of Proinflammatory Cytokines and Chemokines in Lung Tissues

The lung tissue homogenate was obtained by homogenizing tissues in the ice and the total RNA was acquired using Trizol reagent (Life Technologies) following the company supplied protocol. The complementary DNA (cDNA) was acquired by reverse-transcription and then RT-PCR was performed using Thunder Bird SYBR qPCR mix (Toyobo) in a Light cycler 480II instrument (Roche) according to company's instructions. The RNA expression level of cytokine and chemokine was recorded and analyzed using Roche Lightcycler software.

The primer sequences used in real-time PCR were listed in Supplemental Table S1.

Supplemental table S1. The primers for real-time PCR

Primer (mouse)	5'-3'
β -actin F	GCTTCTTTGCAGCTCCTTCGT
β -actin R	CCTTCTGACCCATTCCCACC
IL-1 β F	GGTGTGTGACGTTCCCATTAGAC
IL-1 β R	AGGGTGGGTGTGCCGTCTT
IL-6 F	AGTTGCCTTCTTGGGACTGATG
IL-6 R	TGCAAGTGCATCATCGTTGTTTCAT
TNF α F	GTCTACTGAACTTCGGGGTGATCG
TNF α R	TGGGCTACAGGCTTGTCACTCG
CCL2 F	CAGCCAACTCTCACTGAAGCC
CCL2 R	AACTACAGCTTCTTTGGGACACC

RESULTS

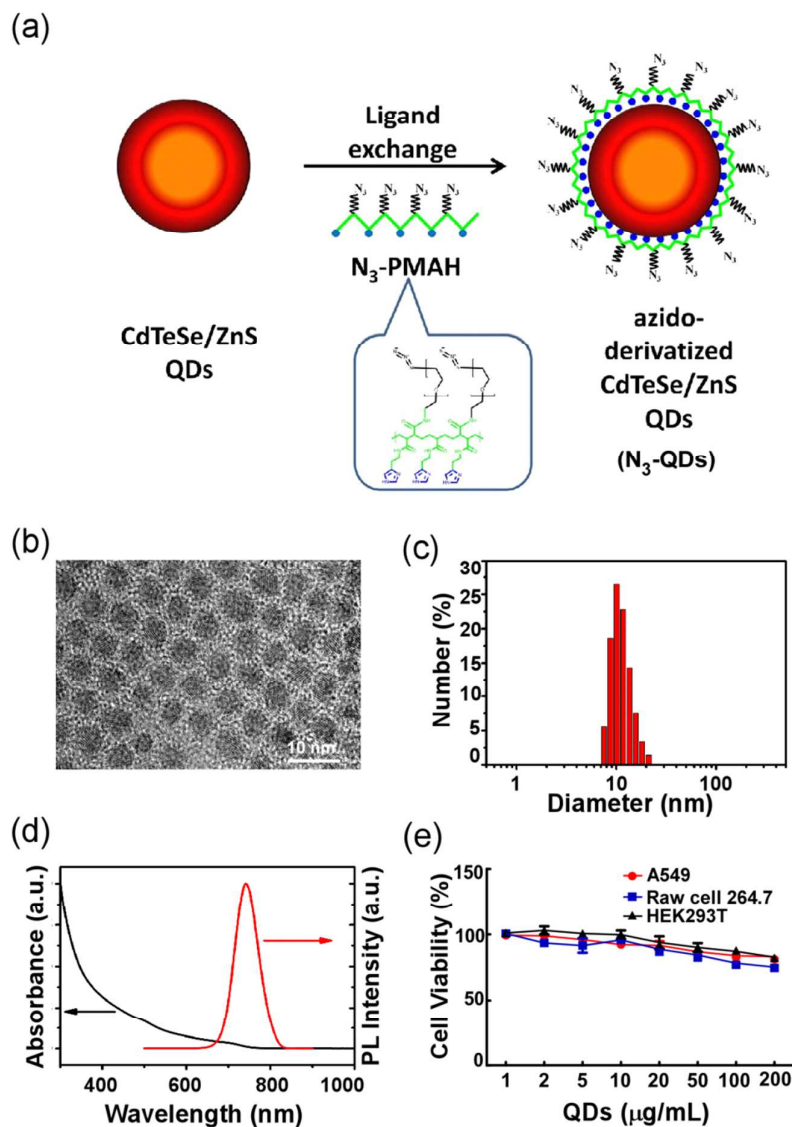


Figure S1. Characterization of azido-derivatized NIR QDs (N_3 -QDs). (a) The schematic diagram of N_3 -QD preparation. (b) Transmission electron microscopy (TEM) images of N_3 -QDs. (c) The hydrodynamic diameter of the N_3 -QDs. (d) Ultraviolet-visible absorbance spectra (black line) and photoluminescence spectra (PL, red line) of N_3 -QDs. (e) The cytotoxicity of N_3 -QDs. A549, Raw 264.7 or HEK293T cells were incubated with 1-200 $\mu g/ml$ of N_3 -QDs for 24 h, and the cell viability was evaluated using MTT. Data shown are mean \pm SE (n= 3–4).

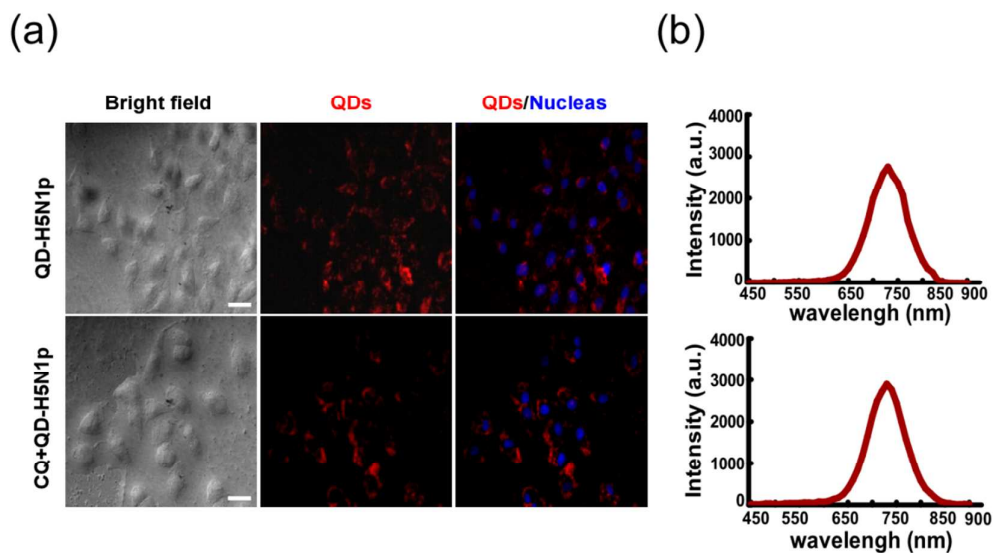


Figure S2. The stability of QDs in the acidic environment (endosome/lysosome). A549 cells were pretreated with or without chloroquine (25 μ M) for 1 h, followed by infection with QD-labeled H5N1p (MOI= 0.5). After 24 h post infection, (a) the fluorescent images and (b) the spectrum of QDs were recorded using multispectral fluorescence microscopy. Scale bar=10 μ m.

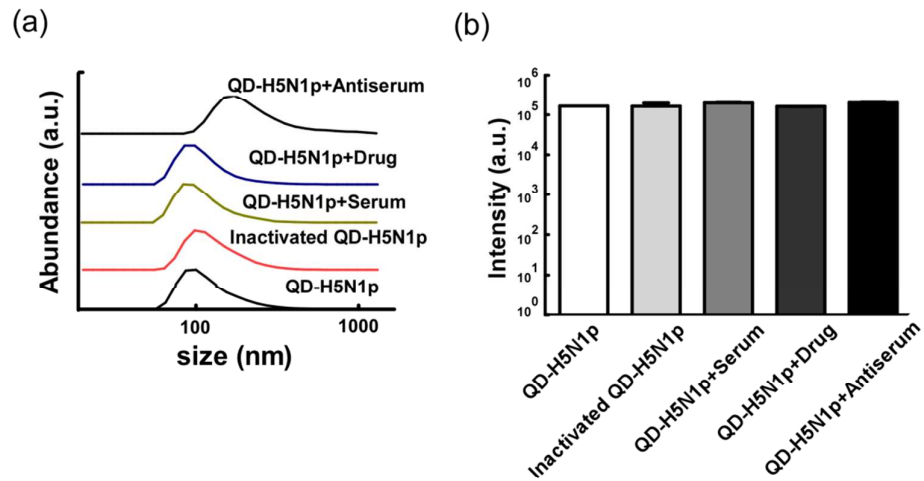


Figure S3. The effect of antiviral agents on the particle size and fluorescent intensity of QD-labeled H5N1 pseudotype virus (H5N1p). QD-labeled H5N1p (QD-H5N1p) was incubated with oseltamivir carboxylate (drug, 8 μ g/ml) or mouse antiserum against H5N1p (antiserum, 1:1000) antibodies at room temperature for 2 h. For comparison, some QD-H5N1p was incubated with control serum from naive mice. Hydrodynamic diameter (a) and fluorescent intensity (b) of QD-H5N1p was measured using Zetasizer Nano ZS instrument and F900 fluorescent spectrometer, respectively. Data shown are mean \pm SE (n= 3–4).

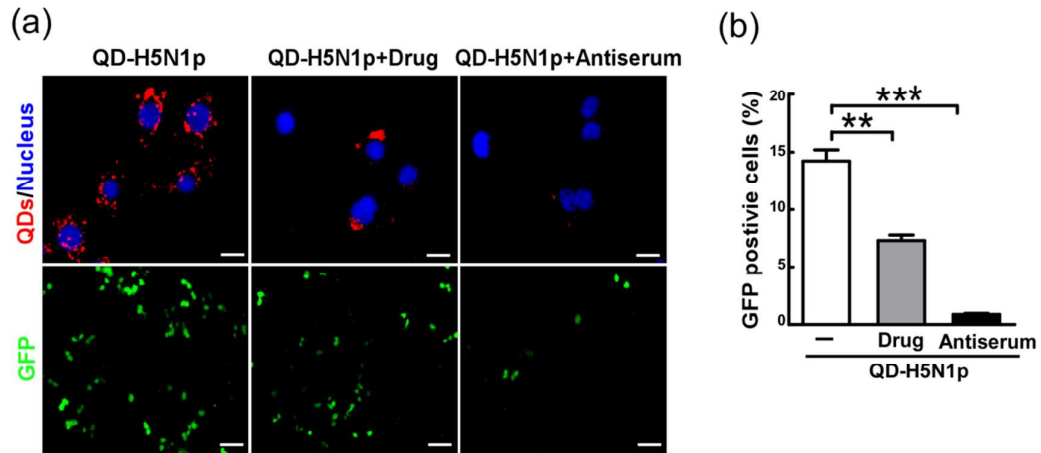


Figure S4. The effect of antiviral agents on the infectivity of QD-H5N1p. (a) The binding of QD-H5N1p on HEK293T cells. HEK 293T cells were infected by QD-H5N1p with or without oseltamivir carboxylate (drug) or mouse antiserum against H5N1p (antiserum) at 37°C for 30 min, and the fluorescent imaging of cells by the multispectral imaging system. Scale bar= 5 μ m. (b) At 24 h post infection, fluorescence images of GFP in cells were recorded with a fluorescence microscopy. Scale bar= 20 μ m. (c) The expression of GFP in virus-infected cells was analyzed using flow cytometry. Bars shown are mean \pm SE (n= 4), and the differences among groups were determined using One-way ANOVA analysis. **: $p<0.01$; ***: $p<0.001$.

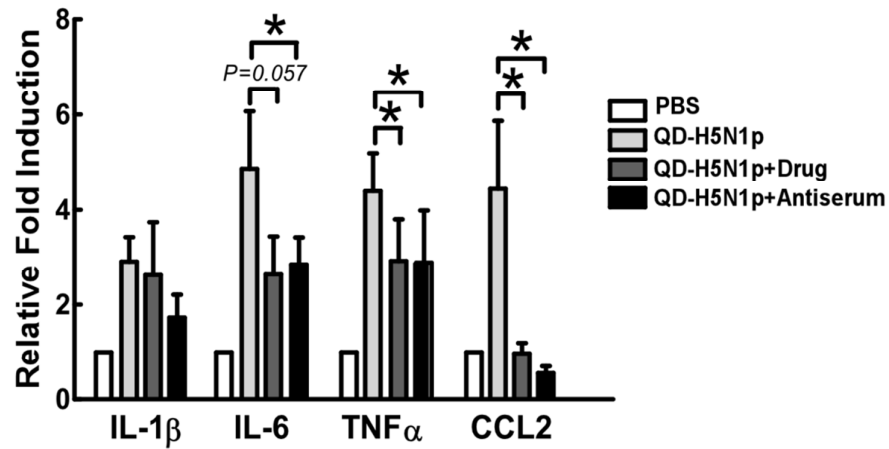


Figure S5. The effect of antiviral agents on proinflammatory cytokines and chemokines induced by QD-H5N1p in lung. Six-week old female Balb/c mice were i.n. infected by PBS or QD-H5N1p \pm oseltamivir carboxylate (drug) or mouse antiserum against H5N1p (antiserum) as described in Methods. The cytokine and chemokine mRNA expression levels in lung tissue were evaluated by real-time qPCR on day 3 post infection. Data shown are mean \pm SEM (n= 5), and the differences between groups were analyzed by one-way ANOVA. *: $p < 0.05$.

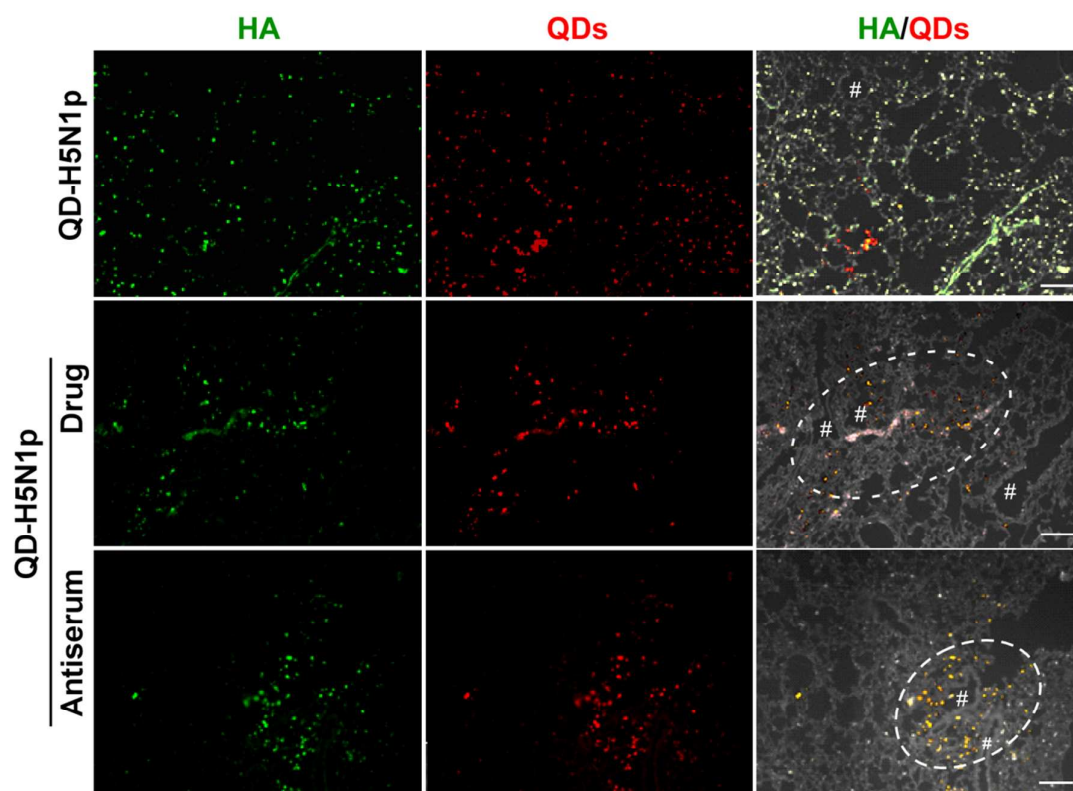


Figure S6. Antiviral agents affect the distribution of QD-H5N1p in lungs. Mice were i.n. infected with QD-H5N1p \pm oseltamivir carboxylate (antiviral drug) or antiserum against H5N1p (Ab) and then sacrificed on day 3 for lung tissue section. The fixed tissue section were stained with anti-HA antibody followed by Alexa 488 conjugated anti-IgG to identify viral particles (green). The images were recorded using a multispectral imaging system. #: Main conducting airways. Dashed circles: H5N1p-accumulated areas. Scale bar= 100 μ m.